NCP-function based dual weighted residual error estimators for Signorini's problem

Andreas Rademacher

Institute of Applied Mathematics, Technische Universität Dortmund

Abstract

In this paper, we consider goal-oriented adaptive finite element methods for Signorini's problem. The basis is a mixed formulation, which is reformulated as nonlinear variational equality using a nonlinear complementarity (NCP) function. For a general discretization, we derive error identities with respect to a possible nonlinear quantity of interest in the displacement as well as the contact forces, which are included as Lagrange multiplier, using the dual weighted residual (DWR) method. Afterwards, a numerical approximation of the error identities is introduced. We exemplify the results for a low order mixed discretization of Signorini's problem. The theorectical findings and the numerical approximation scheme are finally substantiated by some numerical examples.

Keywords: Signorini's problem, mixed finite element method, goal-oriented a posteriori error estimation

1 Introduction

Contact problems play an important role in the modelling of many physical or engineering processes, see for instance [15, 25]. Consequently, the efficient and accurate numerical solution of contact problems has been a focus of research over the last decades. On the one hand efficient solution algorithms are indispensable. On the other hand, adaptive algorithms ensure that a minimal effort is needed to achieve a given error tolerance. The main ingredient of the adaptive algorithm is an accurate a posteriori error estimator. In many applications, one is interested in controlling the error in a user-defined quantity of interest, which in contact problems frequently involves the contact forces. Thus, goal-oriented estimators are often of special interest.

A posteriori error estimators in the energy norm for the obstacle problem are frequently studied in literature. We refer for instance to [1, 3, 10, 13, 21, 24, 29, 39]. Convergence results for adaptive algorithms in the context of obstacle problems are proven in [12, 11, 37]. A posteriori error estimates in the energy norm for Signorini's problem are discussed, e.g., in [14, 19, 28, 34, 40]. Multibody contact problems are considered in [26, 41]. One popular technique for the derivation of a posteriori error estimates with respect to user-defined quantities of interest is the dual weighted residual (DWR) method, cf. [2, 4]. A basic ingredient is the representation of the quantity of interest by the solution of a so-called dual problem. Comparable arguments are used in [30, 31] to derive similar a posteriori error estimates. First results on DWR methods for contact problems are discussed in [7, 8] and are summarized in [38]. They are based on a dual variational inequality and consider linear quantities of interest in the displacement. An alternative approach based on a linear dual problem is presented in [36], where also nonlinear quantities of interest in the displacement are considered. It is extended in [32]. Based on a linear mixed dual problem not depending on the primal problem, the error in quantities of interest in the displacement as well as the Lagrange multiplier, which coincides with the contact forces, are estimated. The later approach also significantly improves the localization of the error estimate. However, in both approaches the contact conditions enter by extra additive terms in the estimate, which consist in some product of the dual solution with the error of the primal solution. In particular, the error in the contact conditions does not directly enter the estimate and the extra terms strongly depend on the numerical approximation of the error in the primal solution. The approach presented in this article overcomes these drawbacks. It is based on a reformulation of Signorini's problem in mixed form as a nonlinear and nonsmooth variational equality using a nonlinear complementarity (NCP) function, see for instance [20]. The arising dual problem is also a linear mixed problem, but it depends on the active and inactive set of the primal contact problem. Applying the DWR framework taking into account the nonsmoothness of the equation leads to the usual error identities. However, the arising remainder terms are of first order in the error of the discrete active set. The discussed numerical results substantiate that the remainder terms can be neglected. The presented analysis applies to a wide range of discretization schemes. The application on mixed discretization schemes like the ones presented in [17, 23] is straight forward. If Newton like methods are used for solving the discrete contact problem, the dual problem coincide with the transposed system of the last Newton step. If displacement based discretization schemes such as [5, 27, 42] are used, an approximation to the Lagrange multiplier has to be constructed in a post processing step, cf. e.g. [10]. Afterwards, a numerical approximation of the error identity depending on the different discretization approaches has to be realized. We exemplify such a strategy for the mixed discretization introduced in [17].

The paper is organized as follows: In Section 2, we introduce the strong and the mixed formulation of Signorini's problem. Furthermore, the assumption on the discretization are formulated. Section 3 focuses on the derivation of the error identities involving the primal as well as the primal and the dual residual. Moreover, the connection between primal und dual residual is clarified. The basic ideas for the numerical approximation of the error identities are explained in Section 4. Afterwards, the ideas are exemplified for a concrete mixed discretization. The numerical results presented in Section 5 substantiate the theoretical findings and the numerical approximation schemes. The paper concludes with a discussion of the results and an outlook on further tasks.

2 Problem formulation

Let $\Omega \subset \mathbb{R}^d$, $d = 2, 3$, be a domain with sufficiently smooth boundary $\Gamma := \partial\Omega$. Moreover, let $\Gamma_D \subset \Gamma$ be closed with positive measure and let $\Gamma_C \subset \Gamma\backslash\Gamma_D$ with $\overline{\Gamma}_C \subsetneq \Gamma\backslash\Gamma_D$. The usual Sobolev spaces are denoted by $L^2(\Omega)$, $H^l(\Omega)$ with $l \geq 1$, and $H^{1/2}(\Gamma_C)$. We set $H^1_D(\Omega) := \left\{ v \in H^1(\Omega) \middle|\, \gamma(v) = 0 \text{ on } \Gamma_D \right\}$ and $V := \left(H^1_D(\Omega)\right)^d$ with the trace operator γ. The space $\tilde{H}^{-1/2}(\Gamma_C)$ denotes the topological dual space of $H^{1/2}(\Gamma_C)$ with the norms $\|\cdot\|_{-1/2,\Gamma_C}$ and $\|\cdot\|_{1/2,\Gamma_C}$, respectively. Let $(\cdot,\cdot)_{0,\omega}$, $(\cdot,\cdot)_{0,\Gamma'}$ be the usual L^2-scalar products on $\omega \subset \Omega$ and $\Gamma' \subset \Gamma$. Note that the linear and bounded mapping $\gamma_C := \gamma_{|\Gamma_C} : H^1_D(\Omega) \to H^{1/2}(\Gamma_C)$ is surjective due to the assumptions on Γ_C, cf. [25, p.88]. For functions in $L^2(\Gamma_C)$, the inequality symbols $\geq$ and $\leq$ are defined as "almost everywhere". We set $H^{1/2}_+(\Gamma_C) := \left\{ v \in H^{1/2}(\Gamma_C) \middle|\, v \geq 0 \right\}$. Furthermore, we define the dual cone of $H^{1/2}_+(\Gamma_C)$ by $\Lambda_n := \left\{ \mu \in \tilde{H}^{-1/2}(\Gamma_C) \middle|\, \forall v \in H^{1/2}_+(\Gamma_C) : \langle \mu, v\rangle \geq 0 \right\}$. For the displacement field $v \in V$, we specify the linearized strain tensor as $\varepsilon(v) := \frac{1}{2}\left(\nabla v + (\nabla v)^\top\right)$ and the stress tensor as $\sigma(v)_{ij} := \sum_{k,l} \mathcal{C}_{ijkl}\varepsilon(v)_{kl}$ describing a linear-elastic material law where $\mathcal{C}_{ijkl} \in L^\infty(\Omega)$ with $\mathcal{C}_{ijkl} = \mathcal{C}_{jilk} = \mathcal{C}_{klij}$ and $\sum_{k,l} \mathcal{C}_{ijkl}\tau_{ij}\tau_{kl} \geq \kappa\tau_{ij}^2$ for $\tau \in L^2(\Omega)^{k\times k}_{\text{sym}}$ and a $\kappa > 0$. In what follows,

n denotes the vector-valued function describing the outer unit normal vector with respect to Γ and t the $k \times (k-1)$-matrix-valued function containing the tangential vectors. We define $\sigma_n := \sigma n$, $\sigma_{nn} := n^\top \sigma n$, $\sigma_{nt,l} := t_l^\top \sigma n$, and $v_n := (\gamma_C(v))^\top n$.

Signorini's problem is to find a displacement field $u \in V \cap H^2(\Omega)$ such that

$$-\operatorname{div}(\sigma(u)) = f \text{ in } \Omega, \quad \sigma_n(u) = b \text{ on } \Gamma_N, \tag{1}$$

$$u_n - g \leq 0, \ \sigma_{nn}(u) \leq 0, \ \sigma_{nn}(u)\,(u_n - g) = 0 \text{ on } \Gamma_C, \tag{2}$$

$$\sigma_{nt}(u) = 0 \text{ on } \Gamma_C, \tag{3}$$

where we assume that $f \in \left(L^2(\Omega)\right)^d$, $b \in \left(L^2(\Gamma_N)\right)^d$ and $g \in H^{1/2}(\Gamma_C)$. Equation (1) is the usual equilibrium equation of linear elasticity with the volume and surface loads f and b. The conditions in (2) describes the geometrical contact: We assume that Γ_C is parameterized by a sufficiently smooth function $\varphi : \mathbb{R}^{d-1} \to \mathbb{R}$ such that, without loss of generality, the geometrical contact condition for a displacement field v in the d-th component is given by $\varphi(x) + v_d(x, \varphi(x)) \leq \psi(x_1 + v_1(x, \varphi(x)), \ldots, x_{d-1} + v_{d-1}(x, \varphi(x)))$ with $x := (x_1, \ldots, x_{d-1}) \in \mathbb{R}^{d-1}$ and a sufficiently smooth function ψ describing the surface of an obstacle. The linearization of this condition gives us $v_n \leq g$ in (2) with $g(x) := (\psi(x) - \varphi(x))\left(1 + (\nabla\varphi(x))^\top \nabla\varphi(x)\right)^{-1/2}$, cf. [25, Chapter 2]. The second condition is a sign condition for the normal contact force describing pressure. The complementarity condition in (2) ensures that pressure only occurs in the case of contact. Here, no friction is considered, which is expressed by (3).

With the symmetric, continuous and V-elliptic bilinear form, due to Korn's inequality,

$$a(w, v) := (\sigma(w), \varepsilon(v))_0$$

on $V \times V$ as well as the continuous linear form $\langle \ell, v \rangle := (f, v)_0 + (b, v_N)_{0,\Gamma_N}$ and using some standard arguments of convex analysis (cf., e.g., [15, 16, 25, 35]), we obtain that the tuple $(u, \lambda_n) \in V \times \Lambda_n$ is a saddle point of the contact problem (1-3) if and only if,

$$a(u, v) + \langle \lambda_n, v_n \rangle = \langle \ell, v \rangle, \tag{4}$$

$$\langle \mu_n - \lambda_n, u_n - g \rangle \leq 0, \tag{5}$$

for all $v \in V$ and all $\mu_n \in \Lambda_n$. Note that a unique solution exists under the presented assumptions. Moreover, the Lagrange multiplier λ_n coincides assuming some additional smoothness properties with the normal contact stress $-\sigma_{nn}(u)$.

The contact conditions expressed in inequality (5) can equivalently be formulated as

$$g - u_n \in H_+^{1/2}(\Gamma_C), \quad \lambda_n \in \Lambda_n, \quad \langle \lambda_n, u_n - g \rangle = 0. \tag{6}$$

Under the assumptions $\mathcal{C}_{ijkl} \in W^{1,\infty}(\Omega)$ and $g \in H^{5/2}(\Gamma_C)$, the solution u is contained in $\left(H^2(\Omega_0)\right)^d$ for every compact subset Ω_0 in $\bar{\Omega} \backslash \{\Gamma_D \cup \Gamma_N\}$, cf. [25, Theorem 6.5]. Then equation (4) implies $\lambda \in L^2(\Gamma_C)$. Now, the contact conditions given in (6) simplify to

$$g - u_n \in H_+^{1/2}(\Gamma_C), \quad \lambda_n \geq 0 \text{ a.e. on } \Gamma_C, \quad \lambda_n (u_n - g) = 0 \text{ a.e. on } \Gamma_C, \tag{7}$$

compare [22, Section 2.1] Using a NCP function, cf., e.g., [22, Chapter 4], these conditions can also be expressed by

$$\lambda_n - \max\{0, \lambda_n + u_n - g\} = 0 \text{ a.e. on } \Gamma_C. \tag{8}$$

Testing equality (8) with an arbitrary function $\mu_n \in L^2(\Gamma_C)$, we obtain

$$C(w)(\mu_n) := (\mu_n, \lambda_n - \max\{0, \lambda_n + u_n - g\})_{0,\Gamma_C} = 0$$

with $w = (u, \lambda_n)$. It should be remarked here that the semilinear form C is not Fréchet differentiable in general. Defining the semilinear form

$$A(w)(\varphi) = a(u, v) + (\lambda_n, v_n)_{0,\Gamma_C} - \langle \ell, v \rangle + C(w)(\mu_n)$$

with $\varphi = (v, \mu_n) \in W := V \times L^2(\Gamma_C)$, Signorini's problem (4-5) is written as the nonlinear problem find $w \in W$ with

$$\forall \varphi \in W : \qquad A(w)(\varphi) = 0.$$

Our a posteriori error analysis is not limited to a special discretization. It applies to all discrete approximations w_h to w, which fulfill the following assumption:

Assumption 1. *The discrete solution w_h is included in a finite dimensional subspace $W_h = V_h \times \Lambda_{n,h}$ of W. Furthermore, equation (4) holds for the discrete solution w_h, i.e.*

$$a(u_h, v_h) + (\lambda_{n,h}, v_{h,n})_{0,\Gamma_C} = \langle l, v_h \rangle \tag{9}$$

for all $v_h \in V_h$.

Remark 2. Equation (9) directly implies Galerkin orthogonality, i.e.

$$a(u - u_h, v_h) + (\lambda_n - \lambda_{n,h}, v_{h,n})_{0,\Gamma_C} = 0 \tag{10}$$

for all $v_h \in V_h$.

Remark 3. Assumption 1 only requires $\Lambda_{n,h} \subseteq L^2(\Gamma_C)$ and not $\Lambda_{n,h} \subseteq \Lambda_n$. Consequently, nonconforming approximations of the Lagrange multiplier are included in the analysis.

3 A posteriori error analysis

In this section we derive a goal oriented a posteriori error estimate based on the DWR method. Here, we are interested in estimating the discretization error w.r.t. a possibly nonlinear quantity of interest $J : W \to \mathbb{R}$, which can involve the displacement u as well as the Lagrange multiplier λ_n. To represent the quantity of interest we employ the following dual problem: Find $z = (y, \xi_n) \in W$ with

$$a(v, y) - b(\xi_n, v) = J'_u(w)(v), \tag{11}$$

$$(\mu_n, y_n)_{0,\Gamma_C} + c(\xi_n, \mu_n) = J'_{\lambda_n}(w)(\mu_n). \tag{12}$$

for all $(v, \mu_n) \in W$ with

$$\begin{aligned} b : L^2(\Gamma_C) \times V \to \mathbb{R}, \qquad b(\omega, v) &:= \int_{\Gamma_C} \omega \chi v_n \, do, \\ c : L^2(\Gamma_C) \times L^2(\Gamma_C) \to \mathbb{R}, \qquad c(\omega, \mu) &:= \int_{\Gamma_C} \omega [1 - \chi] \mu \, do, \\ \chi &:= \begin{cases} 1, & \text{if } \lambda_n + u_n - g > 0, \\ 0, & \text{if } \lambda_n + u_n - g \le 0. \end{cases} \end{aligned}$$

The forms b and c correspond to weighted L^2-scalar products on Γ_C, where the weight is given by the indicator function of the active respectively inactive contact set. However, they are no scalar products anymore, because the indicator function is not greater than zero. Furthermore, we obtain the trivial identity

$$\max\{0, \lambda_n + u_n - g\} = \chi(\lambda_n + u_n - g),$$

which will be frequently used in the following calculations. It should be remarked that the dual problem (11-12) corresponds to $A'(w)((v,\mu),z) = J'(w)(v,\mu)$ if the Fréchet derivative C' of C exists. Let $z_h = (y_h, \xi_{n,h}) \in W_h$ be an approximation to z. Using the introduced notations, we obtain the following error estimate in the primal residual only:

Proposition 4. *Assuming that the second Fréchet derivative of J, $J'' : W \to \mathcal{L}(W, W^*)$, exists and that Assumption 1 is valid, there holds*

$$J(w) - J(w_h) = \rho(w_h)(z - z_h) - C(w_h)(\xi_{n,h}) + \mathcal{R}_J^{(2)} + \mathcal{R}_A^{(2)}, \tag{13}$$

with the primal residual

$$\rho(w_h)(\varphi) := -A(w_h)(\varphi).$$

The remainder terms $\mathcal{R}_J^{(2)}$ and $\mathcal{R}_A^{(2)}$ are given by

$$\begin{aligned} \mathcal{R}_J^{(2)} &= -\int_0^1 J''(w_h + se_w)(e_w, e_w)\, s\, ds, \\ \mathcal{R}_A^{(2)} &= \int_{\Gamma_C} \xi_n e_\chi \left[\lambda_{n,h} + u_{h,n} - g\right] do, \end{aligned}$$

with $e_w = w - w_h$, $e_\chi = \chi - \chi_h$, and

$$\chi_h := \begin{cases} 1, & \text{if } \lambda_{n,h} + u_{h,n} - g > 0, \\ 0, & \text{if } \lambda_{n,h} + u_{h,n} - g \le 0. \end{cases}$$

Remark 5. The term $C(w_h)(\xi_{n,h})$ measures the violation of the contact conditions (7).

Remark 6. By $\mathcal{R}_J^{(2)}$, we obtain the usual remainder term of the DWR method for linear problems with nonlinear quantities of interest, cf. [2, Proposition 6.6]. If J is linear, $\mathcal{R}_J^{(2)}$ vanishes.

Remark 7. The remainder $\mathcal{R}_A^{(2)}$ vanishes, once the analytic active set is exactly resolved by the discrete one. It will be discussed in more details in Section 4.

Proof. The application of the box quadrature rule with its remainder term leads to

$$\begin{aligned} J(w) - J(w_h) &= \int_0^1 J'(w_h + se_w)(e_w)\, ds = J'(w)(e_w) + \mathcal{R}_J^{(2)} \\ &= J'_u(w)(e_u) + J'_{\lambda_n}(w)(e_{\lambda_n}) + \mathcal{R}_J^{(2)} \end{aligned}$$

with $e_u = u - u_h$ and $e_{\lambda_n} = \lambda_n - \lambda_{n,h}$. The definition of the continuous dual problem implies

$$J'_u(w)(e_u) + J'_\lambda(w)(e_{\lambda_n}) = a(e_u, y) - b(\xi_n, e_u) + (e_{\lambda_n}, y_n)_{0,\Gamma_C} + c(\xi_n, e_{\lambda_n}).$$

By Galerkin orthogonality (10), we obtain

$$a(e_u, y) + (e_{\lambda_n}, y_n)_{0,\Gamma_C} = a(e_u, e_y) + (e_{\lambda_n}, e_{y,n})_{0,\Gamma_C} = \langle l, e_y\rangle - a(u_h, e_y) - (\lambda_{n,h}, e_{y,n})_{0,\Gamma_C}. \tag{14}$$

We use the contact conditions and the definition of the dual problem to derive

$$
\begin{aligned}
& c\left(\xi_n, \lambda_n-\lambda_{n,h}\right)-b\left(\xi_n, u-u_h\right) \\
= & \int_{\Gamma_C} \xi_n[1-\chi] e_{\lambda_n}\, do-\int_{\Gamma_C} \xi_n \chi e_{u,n}\, do=\int_{\Gamma_C} \xi_n\left\{e_{\lambda_n}-\chi\left[e_{\lambda_n}+e_u\right]\right\} do \\
= & \int_{\Gamma_C} \xi_n\left[\lambda_n-\chi\left[\lambda_n+u_n-g\right]\right] do-\int_{\Gamma_C} \xi_n\left[\lambda_{n,h}-\chi\left[\lambda_{n,h}+u_{h,n}-g\right]\right] do \\
= & \int_{\Gamma_C} \xi_n\left[\lambda_n-\max\left\{0, \lambda_n+u_n-g\right\}\right] do-\int_{\Gamma_C} \xi_n\left[\lambda_{n,h}-\chi_h\left[\lambda_{n,h}+u_{h,n}-g\right]\right] do \\
& +\int_{\Gamma_C} \xi_n e_\chi\left[\lambda_{n,h}+u_{h,n}-g\right] do \\
= & C(w)\left(\xi_n\right)-C\left(w_h\right)\left(\xi_n\right)+\mathcal{R}_A^{(2)}=-C\left(w_h\right)\left(\xi_n-\xi_{n,h}\right)-C\left(w_h\right)\left(\xi_{n,h}\right)+\mathcal{R}_A^{(2)} .
\end{aligned}
$$

Finally, merging all equations leads to

$$
\begin{aligned}
& J(w)-J\left(w_h\right) \\
= & a\left(u-u_h, y\right)-b\left(\xi_n, u-u_h\right)+\left(\lambda_n-\lambda_{n,h}, y\right)_{0,\Gamma_C}+c\left(\xi_n, \lambda_n-\lambda_{n,h}\right)+\mathcal{R}_J^{(2)} \\
= & \left\langle l, y-y_h\right\rangle-a\left(u_h, y-y_h\right)-\left(\lambda_{n,h}, y_n-y_{h,n}\right)_{0,\Gamma_C}-C\left(w_h\right)\left(\xi_n-\xi_{n,h}\right) \\
& -C\left(w_h\right)\left(\xi_{n,h}\right)+\mathcal{R}_A^{(2)}+\mathcal{R}_J^{(2)} \\
= & \rho\left(w_{hH}\right)\left(z-z_h\right)-C\left(w_h\right)\left(\xi_{n,h}\right)+\mathcal{R}_A^{(2)}+\mathcal{R}_J^{(2)},
\end{aligned}
$$

the assertion. □

To obtain an error identity in the primal and dual residual, we have to specify the dual residual.

Proposition 8. *Let the third Fréchet derivative of J, $J''': W \rightarrow \mathcal{L}(W, \mathcal{L}(W, W^*))$ exist and Assumption 1 hold. Then we have the error representation*

$$
J(w)-J\left(w_h\right)=\frac{1}{2} \rho\left(w_h\right)\left(e_z\right)+\frac{1}{2} \rho^*\left(w_h, z_h\right)\left(e_w\right)-C\left(w_h\right)\left(\xi_{n,h}\right)+\mathcal{R}_J^{(3)}+\mathcal{R}_A^{(3)}, \tag{15}
$$

where

$$
\rho^*\left(w_h, z_h\right)(\varphi):=J'\left(w_h\right)(\varphi)-a\left(v, y_h\right)+b_h\left(\xi_{n,h}, v\right)-\left(\mu_n, y_{h,n}\right)_{0,\Gamma_C}-c_h\left(\xi_{n,h}, \mu_n\right)
$$

with the bilinear forms $b_h: \Lambda_{n,h} \times V_h \rightarrow \mathbb{R}$ and $c_h: \Lambda_{n,h} \times \Lambda_{n,h} \rightarrow \mathbb{R}$ given by

$$
\begin{aligned}
b_h(\omega, v) & :=\int_{\Gamma_C} \omega \chi_h v_n\, do, \\
c_h(\omega, \mu) & :=\int_{\Gamma_C} \omega\left[1-\chi_h\right] \mu\, do .
\end{aligned}
$$

The remainder $\mathcal{R}_J^{(3)}$ is given by

$$
\mathcal{R}_J^{(3)}:=\frac{1}{2} \int_0^1 J'''\left(w_h+s e_w\right)\left(e_w, e_w, e_w\right) s(s-1)\, ds
$$

and the remainder $\mathcal{R}_A^{(3)}$ by

$$
\mathcal{R}_A^{(3)}=\frac{1}{2} \int_{\Gamma_C} e_\chi\left\{\xi_n\left[\lambda_{n,h}+u_{h,n}-g\right]+\xi_{n,h}\left[\lambda_n+u_n-g\right]\right\} do .
$$

Remark 9. The remainder $\mathcal{R}_J^{(3)}$ corresponds to the usual remainder of the DWR method, see [2, Proposition 6.2] and compare Remark 6. If J is linear or quadratic in w, $\mathcal{R}_J^{(3)}$ is zero.

Remark 10. If the analytic active set is exactly resolved by the discrete one, the remainder $\mathcal{R}_A^{(3)}$ vanishes. However, due to the missing regularity of C, it is of the same order in e_χ as $\mathcal{R}_A^{(2)}$.

Proof. Using the Trapezoidal quadrature rule with its remainder term leads to

$$\begin{aligned} J(w) - J(w_h) &= \int_0^1 J'(w_h + s e_w)(e_w)\, ds = \frac{1}{2} J'(w)(e_w) + \frac{1}{2} J'(w_h)(e_w) + \mathcal{R}_J^{(3)} \\ &= \frac{1}{2} J'_u(w)(e_u) + \frac{1}{2} J'_{\lambda_n}(w)(e_{\lambda_n}) + \frac{1}{2} J'_u(w_h)(e_u) + \frac{1}{2} J'_{\lambda_n}(w_h)(e_{\lambda_n}) + \mathcal{R}_J^{(3)}. \end{aligned}$$

Proposition 4 directly implies

$$\begin{aligned} & \frac{1}{2} J'_u(w)(e_u) + \frac{1}{2} J'_{\lambda_n}(w)(e_{\lambda_n}) \\ = \ & \frac{1}{2} \rho(w_h)(e_z) - \frac{1}{2} C(w_h)(\xi_{n,h}) + \frac{1}{2} \int_{\Gamma_C} \xi_n e_\chi [\lambda_{n,h} + u_{h,n} - g]\, do. \end{aligned}$$

The contact conditions together with the definition of the discrete dual problem are used to derive

$$\begin{aligned} & c_h(\xi_{n,h}, e_{\lambda_n}) - b_h(\xi_{n,h}, e_u) = \int_{\Gamma_C} \xi_{n,h} [1 - \chi_h] e_{\lambda_n}\, do - \int_{\Gamma_C} \xi_{n,h} \chi_h e_u\, do \\ = \ & \int_{\Gamma_C} \xi_{n,h} \{ e_\lambda - \chi_h [e_{\lambda_n} + e_u] \}\, do \\ = \ & \int_{\Gamma_C} \xi_{n,h} [\lambda_n - \chi_h [\lambda_n + u_n - g]]\, do - \int_{\Gamma_C} \xi_{n,h} [\lambda_{n,h} - \chi_h [\lambda_{n,h} + u_{h,n} - g]]\, do \\ = \ & \int_{\Gamma_C} \xi_{n,h} [\lambda_n - \chi [\lambda_n + u_n - g]]\, do + \int_{\Gamma_C} \xi_{n,h} e_\chi [\lambda_n + u_n - g]\, do \\ & - \int_{\Gamma_C} \xi_{n,h} [\lambda_{n,h} - \max\{0, \lambda_{n,h} + u_{h,n} - g\}]\, do \\ = \ & \int_{\Gamma_C} \xi_{n,h} [\lambda_n - \max\{0, \lambda_n + u_n - g\}]\, do + \int_{\Gamma_C} \xi_{n,h} e_\chi [\lambda_n + u_n - g]\, do - C(w_h)(\xi_{n,h}) \\ = \ & C(w)(\xi_{n,h}) + \int_{\Gamma_C} \xi_{n,h} e_\chi [\lambda_n + u_n - g]\, do - C(w_h)(\xi_{n,h}) \\ = \ & \int_{\Gamma_C} \xi_{n,h} e_\chi [\lambda_n + u_n - g]\, do - C(w_h)(\xi_{n,h}). \end{aligned}$$

Inserting the Galerkin orthogonality relation (10), the foregoing calculation shows

$$\begin{aligned} & J'_u(w_h)(e_u) + J'_{\lambda_n}(w_h)(e_{\lambda_n}) \\ = \ & J'_u(w_h)(e_u) + J'_\lambda(w_h)(e_{\lambda_n}) - a(e_u, y_h) - (e_{\lambda_n}, y_{h,n})_{0,\Gamma_C} \\ & - c_h(\xi_{n,h}, e_{\lambda_n}) + b_h(\xi_{n,h}, e_u) + \int_{\Gamma_C} \xi_{n,h} e_\chi [\lambda_n + u_n - g]\, do - C(w_h)(\xi_{n,h}) \\ = \ & \rho^*(w_h, z_h)(e_w) + \int_{\Gamma_C} \xi_{n,h} e_\chi [\lambda_n + u_n - g]\, do - C(w_h)(\xi_{n,h}). \end{aligned}$$

All in all, we obtain

$$\begin{aligned}
& J(w) - J(w_h) \\
= \; & \frac{1}{2}\rho(w_h)(e_z) - \frac{1}{2}C(w_h)(e_{\xi_n}) + \frac{1}{2}\int_{\Gamma_C} \xi_n e_\chi [\lambda_{n,h} + u_{h,n} - g] \; do \\
& + \frac{1}{2}\rho^*(w_h, z_h)(e_w) - \frac{1}{2}C(w_h)(\xi_{n,h}) + \frac{1}{2}\int_{\Gamma_C} \xi_{n,h} e_\chi [\lambda_n + u_n - g] \; do + \mathcal{R}_J^{(3)} \\
= \; & \frac{1}{2}\rho(w_h)(e_z) + \frac{1}{2}\rho^*(w_h, z_H)(e_w) - C(w_h)(\xi_{n,h}) + \mathcal{R}_A^{(3)} + \mathcal{R}_J^{(3)}
\end{aligned}$$

and therewith the assertion. □

In the following proposition, we compare the primal and the dual residual:

Proposition 11. *Assume that the second Fréchet derivative of J, $J'' : W \to \mathcal{L}(W, W^*)$, exists and that Assumption 1 is valid. The difference between the primal residual ρ and the dual residual $\rho^\star$ is given by*

$$\rho^\star(w_h, z_h)(w - w_h) = \rho(w_h)(z - z_h) + \Delta J + \Delta C,$$

where

$$\begin{aligned}
\Delta J &= -\int_0^1 J''(w_h + s e_w)(e_w, e_w) \; ds \\
\Delta C &= \int_{\Gamma_C} e_\chi \left\{ e_{\xi_n} [\lambda_n + u_n - g] - \xi_n [e_{\lambda_n} + e_{u,n}] \right\} \; do.
\end{aligned}$$

Remark 12. Proposition 11 says that the difference between the primal and the dual residual is of second order in the error. Thus it is of higher order in the error than the remainder terms $\mathcal{R}_A^{(2)}$ and $\mathcal{R}_A^{(3)}$. Consequently, we cannot use the difference between the primal and dual residual to estimate the remainder $\mathcal{R}_A^{(2)}$ as it is possible for smooth nonlinear problems, cf. [2, Proposition 6.6 and Remark 6.7].

Remark 13. For quantities of interest J, which are linear in w, ΔJ vanishes.

Proof. Starting from the definition of the dual residual $\rho^\star$ and the continuous dual problem, we obtain using (14)

$$\begin{aligned}
& \rho^\star(w_h, z_h)(e_w) \\
= \; & J'(w_h)(e_w) - a(e_u, y_h) + b_h(\xi_{n,h}, e_u) - (e_{\lambda_n}, y_{h,n})_{0,\Gamma_C} - c_h(\xi_{n,h}, e_{\lambda_n}) \\
= \; & J'(w_h)(e_w) - a(e_u, y_h) + b_h(\xi_{n,h}, e_u) - (e_{\lambda_n}, y_{h,n})_{0,\Gamma_C} - c_h(\xi_{n,h}, e_{\lambda_n}) \\
& - J'(w)(e_w) + a(e_u, y) - b(\xi_n, e_u) + (e_{\lambda_n}, y_n)_{0,\Gamma_C} + c(\xi_n, e_{\lambda_n}) \\
= \; & -\int_0^1 J''(w_h + s e_w)(e_w, e_w) \; ds + a(e_u, e_z) + (e_{\lambda_n}, e_{y,n})_{0,\Gamma_C} \\
& + b_h(\xi_{n,h}, e_u) - b(\xi_n, e_u) - c_h(\xi_{n,h}, e_{\lambda_n}) + c(\xi_n, e_{\lambda_n}) \\
= \; & \Delta J + \rho(w_h)(z - z_h) + C(w_h)(e_{\xi_n}) \\
& - [c_h(\xi_{n,h}, e_{\lambda_n}) - b_h(\xi_{n,h}, e_u)] + c(\xi_n, e_{\lambda_n}) - b(\xi_n, e_u).
\end{aligned}$$

From the proof of Proposition 4, we know

$$c(\xi_n, e_{\lambda_n}) - b(\xi_n, e_u) = -C(w_h)(\xi_n) + \int_{\Gamma_C} \xi_n e_\chi [\lambda_{n,h} + u_{h,n} - g] \; do.$$

In the proof of Proposition 8, we have seen

$$c_h(\xi_{n,h}, e_{\lambda_n}) - b_h(\xi_{n,h}, e_u) = -C(w_h)(\xi_{n,h}) + \int_{\Gamma_C} \xi_{n,h} e_\chi [\lambda_n + u_n - g] \, do.$$

These two equations together with the foregoing calculation lead to

$$\begin{aligned}
\Delta C &= C(w_h)(e_{\xi_n}) - [c_h(\xi_{n,h}, e_{\lambda_n}) - b_h(\xi_{n,h}, e_u)] + c(\xi_n, e_{\lambda_n}) - b(\xi_n, e_u) \\
&= C(w_h)(e_{\xi_n}) + C(w_h)(\xi_{n,h}) - \int_{\Gamma_C} \xi_{n,h} e_\chi [\lambda_n + u_n - g] \, do \\
&\quad - C(w_h)(\xi_n) + \int_{\Gamma_C} \xi_n e_\chi [\lambda_{n,h} + u_{h,n} - g] \, do \\
&= \int_{\Gamma_C} \xi_n e_\chi [\lambda_{n,h} + u_{h,n} - g] \, do - \int_{\Gamma_C} \xi_{n,h} e_\chi [\lambda_n + u_n - g] \, do.
\end{aligned}$$

Using

$$\begin{aligned}
& \xi_n [\lambda_{n,h} + u_{h,n} - g] - \xi_{n,h} [\lambda_n + u_n - g] \\
= \; & \xi_n [\lambda_{n,h} - \lambda_n + u_{h,n} - u_n] + \xi_n [\lambda_n + u_n - g] - \xi_{n,h} [\lambda_n + u_n - g] \\
= \; & -\xi_n [e_\lambda + \gamma_n(e_u)] + e_\xi [\lambda_n + \gamma_n(u) - g]
\end{aligned}$$

finishes the proof. □

4 Numerical evaluation of the error identities

The error identities (13) and (15) from Proposition 4 and 8 cannot be evaluated numerically, since they involve the analytic solutions w and z as well as the remainder terms are unknown. The remainder terms $\mathcal{R}_J^{(2)}$ and $\mathcal{R}_J^{(3)}$ are of second and third order in the error, respectively. Thus they are of higher order and can be neglected. The remainder terms $\mathcal{R}_A^{(2)}$ and $\mathcal{R}_A^{(3)}$ are first order in the error in the active set. Numerical experiments show that this error is fast decreasing. However, a strict mathematical analysis of the convergence order of $\mathcal{R}_A^{(2)}$ and $\mathcal{R}_A^{(3)}$ is an open question and depends on the chosen discretization. The numerical results in Section 5 substantiate that it is possible to neglect also $\mathcal{R}_A^{(2)}$ and $\mathcal{R}_A^{(3)}$. Furthermore, we have to numerically approximate w and z. The corresponding operator is called $\mathcal{A}$, which is discretization dependent. We refer to [2, Section 4.1 and Section 5.2] for an overview of possible choices and their mathematical justification under strong smoothness assumptions. All in all, we obtain the primal error estimator

$$J(w) - J(w_h) \approx \eta_p := \rho(w_h)(\mathcal{A}(z_h) - z_h) - C(w_h)(\xi_{n,h})$$

and the primal dual one

$$J(w) - J(w_h) \approx \eta := \frac{1}{2}\rho(w_h)(\mathcal{A}(z) - z_h) + \frac{1}{2}\rho^*(w_h, z_h)(\mathcal{A}(w_h) - w_h) - C(w_h)(\xi_{n,h}).$$

Up to now, the complete analysis has been developed for a general discretization. Henceforth, we concretize the results for a mixed discretization, which was first proposed in [17] and extended to higher order methods in [35]. However, we solve the discrete problems by a primal-dual-active-set-strategy, see [6], in contrast to the Schur-complement approach in the mentioned references. To be precise, let $\mathcal{T}_h$ be a finite element mesh of Ω with mesh size h and let $\mathcal{E}_C$ be a finite element mesh of Γ_C with mesh size H, respectively. The number of mesh elements in $\mathcal{T}_h$ is denoted by M_Ω and in $\mathcal{E}_C$ by M_C. We use line segments, quadrangles or hexahedrons to define $\mathcal{T}$ or $\mathcal{E}_C$. But this is not a restriction, triangles and tetrahedrons are also possible. Furthermore, let $\Psi_T : [-1,1]^d \to T \in \mathcal{T}_h$ and $\Phi_E : [-1,1]^{d-1} \to E \in \mathcal{E}_C$ be affine and d-linear transformations. We define

$$\begin{aligned} V_h &:= \left\{ v \in V \,\middle|\, \forall T \in \mathcal{T}_h : \; v_{i|T} \circ \Psi_T \in Q_1 \right\}, \\ \Lambda_{n,H} &:= \left\{ \mu \in L^2(\Gamma_C) \middle| \; \forall E \in \mathcal{E}_C : \; \mu_{|E} \circ \Phi_E \in \mathbb{P}_0, \, \mu_E \geq 0 \right\}, \end{aligned}$$

where Q_1 is the set of d-linear functions on $[-1,1]^d$ and $\mathbb{P}_0$ the set of piecewise constant basis functions for the Lagrange Multiplier on $[-1,1]^{d-1}$. The discrete saddle point problem is to find $(u_h, \lambda_{n,H}) \in V_h \times \Lambda_{n,H}$ such that

$$\forall v_h \in V_h : \qquad a(u_h, v_h) + (\lambda_{n,H}, v_{h,n})_{0,\Gamma_C} = \langle l, v_h \rangle, \tag{16}$$

$$\forall \mu_{n,H} \in \Lambda_{n,H} : \qquad (\mu_{n,H} - \lambda_{n,H}, u_{h,n} - g)_{0,\Gamma_C} \leq 0. \tag{17}$$

It is well-known, that there exists a unique discrete saddle point $(u_h, \lambda_{n,H}) \in V_h \times \Lambda_{n,H}$, if a discrete inf-sup condition is fulfilled. In the case of quasi-uniform meshes the discrete inf-sup condition holds if the quotient of the mesh sizes h/H is sufficiently small, cf. [18]. It is noted that different mesh sizes h and H implies that the Lagrange multiplier is defined on a coarser mesh which may lead to a higher implementational complexity than using a surface mesh $\mathcal{E}_C$ which is inherited from the interior mesh $\mathcal{T}_h$. In compliance with the mentioned reference, we observe in our experiments that the choice $H = h$ leads to oscillating Lagrange multipliers whereas $H = 2h$ results in a stable scheme. Thus, we use meshes with $H = 2h$ in the experiments of Section 5.

To motivate our definition of the discrete dual solution, we give here the details of the solution algorithm, cf. [6, Section 5.4.1]. We begin with a reformulation of the contact conditions (17):

$$\begin{aligned} \int_{\Gamma_C} (u_{h,n} - g)\psi_H \; do &\leq 0, \\ \int_{\Gamma_C} \lambda_{n,H}\psi_H \; do &\geq 0, \\ \int_{\Gamma_C} \lambda_{n,H}\psi_H \; do \int_{\Gamma_C} (u_{h,n} - g)\psi_H \; do &= 0, \end{aligned} \tag{18}$$

which have to hold for all $\psi_H \in \Lambda_{n,H}$. We specify the coupling matrix $N \in \mathbb{R}^{M_C \times \bar{M}}$ with respect to the bases of $V_h = \langle \phi_1, \dots, \phi_{\bar{M}} \rangle$ and $\Lambda_{n,H} = \langle \psi_1, \dots, \psi_{M_C} \rangle$ by

$$N_{ij} := \int_{\Gamma_C} \psi_i(\phi_j) \cdot n \; do,$$

the mass matrix $M \in \mathbb{R}^{M_C \times M_C}$ of the Lagrange Multiplier

$$M_{ij} := \int_{\Gamma_C} \psi_j \psi_i \; do,$$

and the gap vector $\bar{g} \in \mathbb{R}^{M_C}$

$$\bar{g}_i = \int_{\Gamma_C} g\psi_i \; do \; .$$

By a bar, we denote the vector-valued representation of the corresponding discrete function in the belonging basis. The contact conditions (18) read in algebraic form

$$N\bar{u}_h - \bar{g} \leq 0, \; M\bar{\lambda}_{n,H} \geq 0, \; \left(M\bar{\lambda}_{n,H}\right)_i (N\bar{u}_h - \bar{g})_i = 0 \; \forall i = 1, \dots, M_C \; . \tag{19}$$

Using the NCP function

$$C_N(\bar{u}_h, \bar{\lambda}_{n,H})_i := (M\bar{\lambda}_{n,H})_i - \max\left\{0,\ (M\bar{\lambda}_{n,H})_i + c_n(N\bar{u}_h - \bar{g})_i\right\}$$

with a positive constant c_n, the weak contact conditions (19) are equivalently expressed by

$$C_N(\bar{u}_h, \bar{\lambda}_{n,H}) = 0\ . \tag{20}$$

Define the characteristical function χ_i by

$$\chi_i := \begin{cases} 1 & ,\ \left(M\bar{\lambda}_{n,H} + c_n(N\bar{u}_h - \bar{g})\right)_i > 0, \\ 0 & ,\ \left(M\bar{\lambda}_{n,H} + c_n(N\bar{u}_h - \bar{g})\right)_i \le 0. \end{cases}$$

The generalized derivative of the NCP function with variations $\bar{\delta u}_h, \bar{\delta\lambda}_{n,H}$ is then given by

$$C_N'(\bar{u}_h, \bar{\lambda}_{n,H})(\bar{\delta u}_h, \bar{\delta\lambda}_{n,H})_i = -\chi_i\left(-M\bar{\delta\lambda}_{n,H} + c_n N\bar{\delta u}_h\right)_i - \left(M\bar{\delta\lambda}_{n,H}\right)_i .$$

In order to solve (20), we use a semi-smooth Newton's method

$$C_N'\left(\bar{u}_h^{k-1}, \bar{\lambda}_{n,H}^{k-1}\right)\left(\bar{\delta u}_h^{k}, \bar{\delta\lambda}_{n,H}^{k}\right) = -C_N\left(\bar{u}_h^{k-1}, \bar{\lambda}_{n,H}^{k-1}\right),$$

where the new iterates are calculated by $\bar{u}_h^k := \bar{u}_h^{k-1} + \bar{\delta u}_h^k$ and $\bar{\lambda}_{n,H}^k := \bar{\lambda}_{n,H}^{k-1} + \bar{\delta\lambda}_{n,H}^k$. The active and inactive indices in Newton step k are determined by

$$\mathcal{A}_n^k := \left\{i \in \{1,\dots,M_C\}\ \middle|\ \left(M\bar{\lambda}_{n,H} + c_n(N\bar{u}_h - \bar{g})\right)_i > 0\right\} \tag{21}$$

$$\mathcal{I}_n^k := \left\{i \in \{1,\dots,M_C\}\ \middle|\ \left(M\bar{\lambda}_{n,H} + c_n(N\bar{u}_h - \bar{g})\right)_i \le 0\right\}\ . \tag{22}$$

Then the new iterate $\left(\bar{u}_h^k, \bar{\lambda}_{n,H}^k\right)$ of Newton's method is given by the solution of the linear system

$$\begin{aligned} K\bar{u}_h^k + N^\top\bar{\lambda}_{n,H}^k &= \bar{f}, \\ (N\bar{u}_h^k)_i &= \bar{g}_i,\ i \in \mathcal{A}_n^k, \\ (M\bar{\lambda}_{n,H}^k)_i &= 0,\ \ i \in \mathcal{I}_n^k, \end{aligned}$$

with the symmetric and positive definit stiffness matrix $K \in \mathbb{R}^{\bar{M}\times\bar{M}}$ and the load vector $\bar{f} \in \mathbb{R}^{\bar{M}}$. Using a suitable numbering, it corresponds to a saddle point problem of the form

$$\begin{pmatrix} K & \tilde{N}_k^\top & \hat{N}_k^\top \\ \tilde{N}_k & 0 & 0 \\ 0 & 0 & \tilde{M}_k \end{pmatrix}\begin{pmatrix} \bar{u}_h^k \\ \bar{\lambda}_{n,H}^k \end{pmatrix} = \begin{pmatrix} \bar{f} \\ \tilde{g}_k \\ 0 \end{pmatrix},$$

where $\tilde{N}_k$, $\hat{N}_k$ and $\tilde{M}_k$ are submatrices of N and M specified by $\mathcal{A}_n^k$ and $\mathcal{I}_n^k$ as well as $\tilde{g}_k$ a subvector of $\bar{g}$.

The discrete dual solution $z_h = (y_h, \xi_{n,H})$ is defined by the transposed system of the last Newton step, i.e.

$$\begin{pmatrix} K & \tilde{N}_k^\top & 0 \\ \tilde{N}_k & 0 & 0 \\ \hat{N}_k & 0 & \tilde{M}_k \end{pmatrix}\begin{pmatrix} \bar{y}_h \\ \bar{\xi}_{n,H} \end{pmatrix} = \begin{pmatrix} \bar{J}_u \\ \bar{J}_{\lambda_n} \end{pmatrix}.$$

Here, $\bar{J}_u$ represents the assembled vector of $J_u'(w_h)(\phi)$ and $\bar{J}_{\lambda_n}$ the one of $J_{\lambda_n}'(w_h)(\psi)$.

We consider higher order reconstructions of the discrete solutions for the approximation of w and z. This approach is computionally cheaper than to calculate higher order solutions.

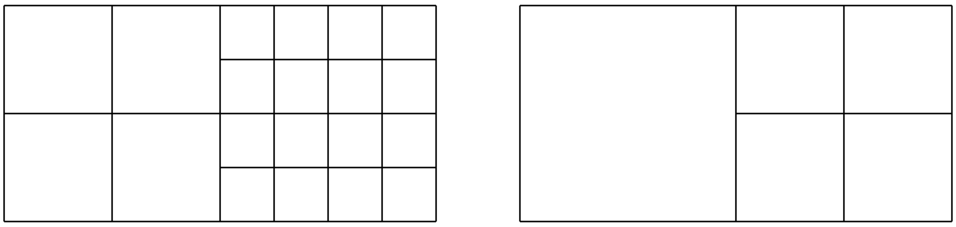

(a) Mesh with patch structure (b) Corresponding patch mesh

Fig. 1: Illustration of the patch structure of the finite element mesh

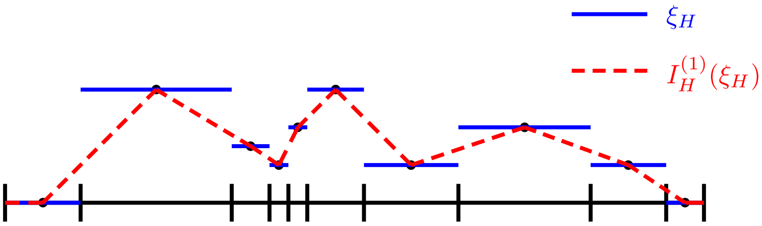

Fig. 2: Illustration of $i_{2H}^{(1)}$

We approximate u and y using patchwise d-quadratic reconstruction, cf., e.g., [2, Section 4.1] for this well known procedure. Let $i_{2h}^{(2)}$ be the corresponding interpolation operator. For the evaluation of $i_{2h}^{(2)}$, a special structure of the adaptively refined finite element mesh is required. This so-called patch-structure is obtained through the refinement of all sons of a refined element, provided that one of these sons is actually marked for refinement. It is illustrated in Figure 1. For the higher order interpolation of the Lagrange multipliers, we use a patchwise linear interpolation $i_{2H}^{(1)}$, it is illustrated in Figure 2. We define $\mathcal{A}^I\left((v_h, \mu_{n,H})\right) := \left(i_{2h}^{(2)} v_h, i_{2H}^{(1)} \mu_{n,H}\right)$ and obtain the error estimators

$$\begin{aligned}
\eta_p &:= \rho\left(w_h\right)\left(\mathcal{A}^I\left(z_h\right) - z_h\right) - C\left(w_h\right)\left(\xi_{n,h}\right), \\
\eta &:= \frac{1}{2}\rho\left(w_h\right)\left(\mathcal{A}^I\left(z_h\right) - z_h\right) + \frac{1}{2}\rho^*\left(w_h, z_h\right)\left(\mathcal{A}^I\left(w_h\right) - w_h\right) - C\left(w_h\right)\left(\xi_{n,h}\right).
\end{aligned}$$

To utilize the error estimators η_p and η in an adaptive refinement strategy, we have to localize the error contributions given by the residuals with respect to the single mesh elements $T \in \mathcal{T}_h$ leading to local error indicators η_T . Here, the filtering technique developed in [9] is applied, which implies less implementational effort than the standard approach using integration by parts outlined for instance in [2]. An alternative localization method was recently proposed in [33]. The terms connected to C are added to the adjacent volume cells to the boundary cells.

5 Numerical results

In this section, we test the theoretical findings by some examples and substantiate the numerical approximation techniques.

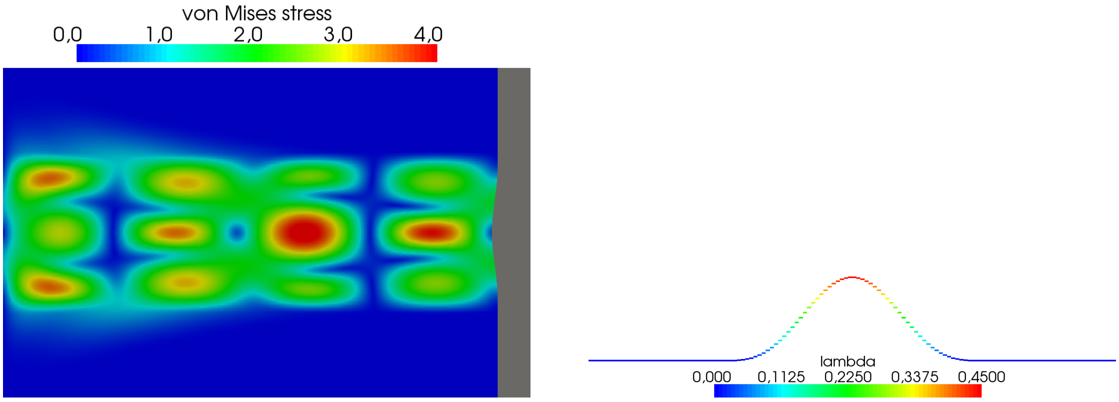

(a) Plot of u_h in Ω and the obstacle

(b) $\lambda_{n,H}$

Fig. 3: Numerical solution of the first 2D example for $M_\Omega = 24576$ and $M_C = 64$

M_Ω	L	$E_{\text{rel}}(J_{a,1})$	$I_{\text{eff}}(J_{a,1}, \eta_p)$	$I_{\text{eff}}(J_{a,1}, \eta)$
384	0	$2.57243 \cdot 10^{-2}$	0.91869	0.38317
1536	1	$1.36313 \cdot 10^{-2}$	1.60751	0.99145
6144	2	$3.76048 \cdot 10^{-3}$	1.02681	1.01653
24576	3	$9.49684 \cdot 10^{-4}$	1.00536	1.00546
98304	4	$2.37789 \cdot 10^{-4}$	1.00134	1.00137
393216	5	$5.94706 \cdot 10^{-5}$	1.00034	1.00034
1572864	6	$1.48691 \cdot 10^{-5}$	1.00008	1.00008

Tab. 1: Results of the presented error estimators for $J_{a,1}$

5.1 First example: Known analytical solution

At first, we consider a 2D Signorini problem with known analytical solution, see also [32]. The domain is given by $\Omega := (-3, 0) \times (-1, 1)$, where homogeneous Dirichlet boundary conditions are prescribed on $\Gamma_D := \{-3\} \times [-1, 1]$ and homogeneous Neumann boundary conditions on $\Gamma_N := (-3, 0) \times \{-1, 1\}$. The possible contact boundary is denoted by $\Gamma_C := \{0\} \times [-1, 1]$. As material law, we apply Hooke's law with Young's modulus $E := 10$ and Poisson number $\nu := 0.3$ using the plain strain assumption. By L the number of uniform refinements based on a coarse initial triangulation is denoted. The analytical solution is called $u(x, y) := (u_1(x, y), u_2(x, y))^\top$, where

$$
\begin{aligned}
u_1(x,y) &:= \begin{cases} -(x+3)^2\left(y - \frac{x^2}{18} - \frac{1}{2}\right)^4\left(y + \frac{x^2}{18} + \frac{1}{2}\right)^4, & |y| < \frac{x^2}{18} + \frac{1}{2}, \\ 0, & \text{else}, \end{cases} \\
u_2(x,y) &:= \begin{cases} \frac{27}{\pi} \sin\left(\frac{4\pi(x+3)}{3}\right)\left[\left(y - \frac{1}{2}\right)^3\left(y + \frac{1}{2}\right)^4 + \left(y - \frac{1}{2}\right)^4\left(y + \frac{1}{2}\right)^3\right], & |y| < \frac{1}{2}, \\ 0, & \text{else}. \end{cases}
\end{aligned}
$$

The volume force is then given by $f := -\operatorname{div}(\sigma(u))$ and the obstacle by $g(y) := u_1(0, y)$. The discrete solution w_h is illustrated in Figure 3.

First, we consider the quantities of interest

$$
\begin{aligned}
J_{a,1}(u) &:= \int_\Omega \omega_{-0.5}(x) \|u\|^2 \, dx, \\
J_{a,2}(\lambda_n) &:= \int_{-1}^{1} \left(0.5 \tanh\left(20(0.25 - |y - 0.125|)\right) + 0.5\right) \lambda_n^2(y) \, dy,
\end{aligned}
$$

where $\omega_m(x) = 0.5\left(\tanh(20(d - |x - (m, 0)|_2)) + 1\right)$ is a cut off function w.r.t. the disc $B_d((m, 0))$, $d = 0.5$ and $m \in [-3, 0]$. The relative discretization error w.r.t. the quantity of

M_Ω	L	$E_{\text{rel}}(J_{a,2})$	$I_{\text{eff}}(J_{a,2},\eta_p)$	$I_{\text{eff}}(J_{a,2},\eta)$
384	0	$9.59089 \cdot 10^{-2}$	1.13982	0.14453
1536	1	$2.50765 \cdot 10^{-1}$	1.17490	0.85087
6144	2	$5.50751 \cdot 10^{-2}$	1.06133	0.95967
24576	3	$1.32901 \cdot 10^{-2}$	1.08439	0.99017
98304	4	$3.29218 \cdot 10^{-3}$	1.09121	0.99752
393216	5	$8.21155 \cdot 10^{-4}$	1.09293	0.99938
1572864	6	$2.05171 \cdot 10^{-4}$	1.09337	0.99984

Tab. 2: Results of the presented error estimators for $J_{a,2}$

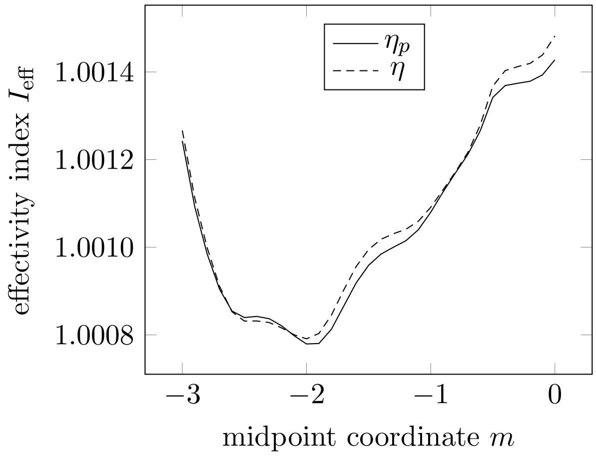

Fig. 4: Plot of the effectivity indices in depence of the midpoint of the quantity of interest m for $M_\Omega = 98304$

interest is given by

$$E_{\text{rel}}(J) := \frac{|J(u,\lambda_n) - J(u_h,\lambda_{n,H})|}{|J(u,\lambda_n)|},$$

and the effectivity index by

$$I_{\text{eff}}(J,\tilde{\eta}) := \frac{J(u,\lambda_n) - J(u_h,\lambda_{n,H})}{\tilde{\eta}}.$$

In Table 1, the results for the quantity of interest $J_{a,1}$ are listed. We found by analyzing the data that the effectivity indices seem to converge of order h^2 to 1 for η_p and η, which is almost optimal. When regarding $J_{a,2}$, see Table 2, we observe an almost constant effectivity index of 1.09 for η_p. However, the effectivity index is very good. In contrast to η_p, the effectivity index for η seems to converges to 1 with order h^2. From the numerical experiments in [32], we know that $i_{2H}^{(1)}\lambda_{n,H}$ is not of higher order in the integral over Γ_C. But, in this approach, the contribution of the terms involving $i_{2H}^{(1)}$ is so small that we could not observe this behavior on the considered meshes. Consequently, we obtain an accurate but not asymptotic exact error estimator. It is one advantage of this approach that it is sufficient to work with the higher order reconstruction to obtain reasonable results.

To substantiate this result even more, we consider the quantity of interest

$$J_{a,m}(u) := \int_\Omega \omega_m(x)\|u\|^2\,dx$$

for $m \in [-3,0]$. The effectivity indices of η and η_p in dependence of m are depicted in Figure 4. We obtain effectivity indices in the range of 1.0008 to 1.0014. Thus, the estimate is very

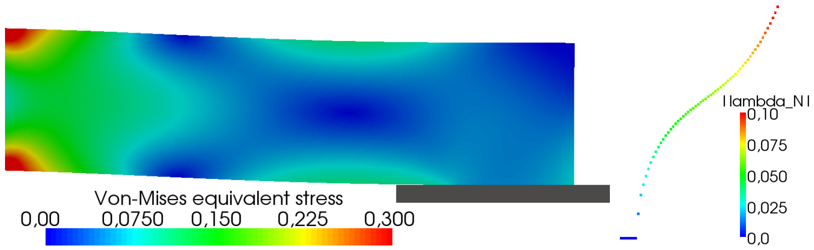

(a) Plot of u_h in Ω and the obstacle (b) $\lambda_{n,H}$

Fig. 5: Numerical solution of the second 2D example for $M_\Omega = 65536$ and $M_C = 64$

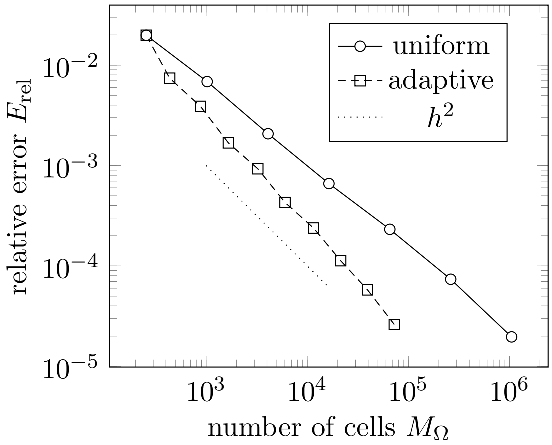

Fig. 6: Comparison of adaptive and uniform refinement

accurate on the one hand and on the other hand there is no real depence on m. In contast to this, the estimators developed in [32] show, if higher order reconstruction is used, a strong dependence on m. There, the effectivity indices become worse for m approach zero.

5.2 Second example: Adaptivity

In the last section, we have examined the accuracy of the error estimator. Now, we address adaptive refinement based on η. We set $\Omega := (0, 0.05) \times (0, 0.2)$, $\Gamma_D := [0, 0.05] \times \{0\}$, $\Gamma_C := \{0.05\} \times [0.15, 0.2]$, and $\Gamma_N := \partial\Omega \backslash (\Gamma_C \cup \Gamma_D)$. We apply Hooke's law under the plain stress assumption with modulus of elasticity $E := 10$ and Poisson ratio $\nu := 0.33$. The volume force is constant and given by $f := (0.5, 0)^\top$. The gap function is also constant, $g := 0.005$. The solution is illustrated in Figure 5. We show the von-Mises equivalent stress

$$\sigma_{M,2}(\sigma, \sigma_e) := \frac{\sqrt{\sigma_{11}^2 + \sigma_{22}^2 + 3\sigma_{21}^2}}{\sigma_e}$$

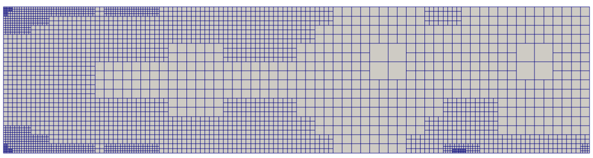

Fig. 7: Adaptive mesh in the 5th iteration

M_Ω	L	E_{rel}	I_{eff}
256	0	$1.98594 \cdot 10^{-2}$	1.26467
436	1	$7.41959 \cdot 10^{-3}$	1.96084
880	2	$3.88619 \cdot 10^{-3}$	1.39197
1660	3	$1.68179 \cdot 10^{-3}$	1.14467
3244	4	$9.29281 \cdot 10^{-4}$	1.28651
6028	5	$4.28825 \cdot 10^{-4}$	1.07428
11536	6	$2.38628 \cdot 10^{-4}$	1.01518
21388	7	$1.12832 \cdot 10^{-4}$	1.08988
39448	8	$5.77479 \cdot 10^{-5}$	0.09065
72604	9	$2.60956 \cdot 10^{-5}$	0.13039

Tab. 3: Detailed results of the adaptive algorithm for the second example

with $\sigma_e := 1$. We have three different sources of large error in this example: Stress peaks in the left corners of the domain, where the Dirichlet boundary conditions change to Neumann boundary conditions as well as the transition zone of contact to non-contact. All these three regions have to be resolved by the adaptive algorithm. We choose $J(u) := \int_B \nabla u : \nabla u \, dx$ with $B = [0, 0.05]^2$ as quantity of interest. Here, B corresponds to the left end of the bar. At first, we solve this problem based on a uniform mesh refinement and obtain a reference value $J_{\text{ref}} = 5.934693870188204 \cdot 10^{-6}$ by extrapolation over all calculated values of J. We use J_{ref} to determine the relative error E_{rel} approximately. The error on the different meshes is plotted in Figure 6, where we do not recover the optimal order of convergence. Afterwards, an adaptive algorithm based on η and a fixed fraction strategy with 0.2% refinement fraction, which is used for comparison with the results in [32], where the same example is considered, is employed. In Figure 6, we observe that the adaptive algorithm reaches the optimal order of convergence as expected. The adaptive mesh in the 5^{th} iteration of the adaptive algorithm is depicted in Figure 7. We observe strong adaptive refinements in the left corners of the domain and on the left end of the active contact zone, which matches our expectations. The adaptive mesh generated based on η is very similar to the ones created by the error estimator based on the mixed dual problem in [32]. The details of the adaptive algorithm are outlined in Table 3. We observe very good effectivity indices up to the last iterates. Since the convergence rate also accelerates in the last iterates, the calculated error seems to be too small due to the used reference value.

5.3 Third example: Three-dimensional

Finally, we consider an example in three dimensions. The domain Ω is given by

$$\Omega := \left\{ x \in \mathbb{R}^3 \middle| \, 0 < x_1 < 0.25, \, 0 < x_2, \, x_3 < 1 \right\}.$$

We assume homogeneous Dirichlet boundary conditions on $\Gamma_D := \{x \in \partial\Omega \,|\, x_1 = 0\}$. As possible contact zone, we choose $\Gamma_C := \{x \in \partial\Omega \,| x_1 = 0.25, \, 0 \leq x_2, \, x_3 \leq 0.5\}$. On the remaining boundary $\Gamma_N = \partial\Omega \backslash (\Gamma_C \cup \Gamma_D)$, homogeneous Neumann boundary conditions are presribed. Here, we use Hook's law with the material parameters $E := 10^5$ and $\nu := 0.3$ and apply no volume or surface loads. The obstacle is parametrized with $z(x) = \sqrt{(x_2 - 0.25)^2 + (x_3 - 0.25)^2}$ by

$$\psi(x) := \begin{cases} 0.25 + 0.05 \left(65536 z^8 - 1 \right), & z \leq 0.25, \\ 0.25, & \text{else.} \end{cases}$$

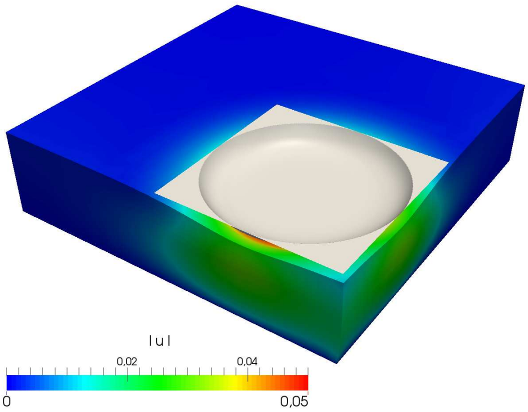

(a) Numerical solution

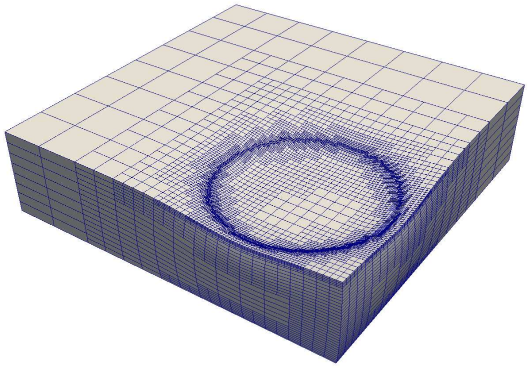

(b) Adaptive mesh

Fig. 8: Plot of the numerical solution of the 3d example on an adaptive mesh with 43688 cells in the 7^{th} iteration of the adaptive algorithm

The numerical solution is illustrated in Figure 8. As the quantity of interest, we choose the functional

$$J(u, \lambda_n) := 10^{-3} \int_B \sigma(u) : \sigma(u)\, dx + \int_{\Gamma_C} \lambda_n\, ds$$

with $B := \{x \in \Omega \,|\, 0 \leq x_1 \leq 0.25,\, 0.625 \leq x_2,\, x_3 \leq 0.875\}$. The adaptive mesh with 43688 cells in the 7^{th} iteration of the adaptive algorithm is also illustrated in Figure 8. We observe mainly refinements at the boundary of the active contact zone. In this example, the term $C(w_h)(\xi_{n,H})$ is comparatively large in the first iterations and then fast decreasing.

6 Conclusions and outlook

In this article, we have presented a new approach to goal oriented a posteriori error estimation in contact problems. The main advantages compared to other methods are that the numerical evaluation by higher order reconstruction methods is not asymptotically exact but accurate that the error in the contact conditions of the discretization scheme is directly measured and that the dual problem is linear. On the other hand, we obtain a remainder term, which we cannot control analytically. This is a topic of further research. The direct measurement of the error in the contact conditions is crucial for two planned extension. This property is necessary for an accurate goal oriented adaptive scheme in dynamic contact problems, where the precise resolution of the impact points is very important. Furthermore, it provides the opportunity to construct model adaptive algorithms, e.g. for switching between linear and nonlinear contact conditions.

Acknowledgement

The author gratefully acknowledges the financial support by the German Research Foundation (DFG) within the subproject A5 of the transregional collaborative research centre (Transregio) 73 “Sheet-Bulk-Metal-Forming”.

References

[1] M. Ainsworth, J. Oden, and C. Lee. Local a posteriori error estimators for variational inequalities. *Numer. Methods Partial Differ. Equ.*, 9:23–33, 1993.

[2] W. Bangerth and R. Rannacher. *Adaptive finite element methods for differential equations*. Lectures in Mathematics, ETH Zürich. Birkhäuser, Basel, 2003.

[3] S. Bartels and C. Carstensen. Averaging techniques yield reliable a posteriori finite element error control for obstacle problems. *Numer. Math.*, 99(2):225–249, 2004.

[4] R. Becker and R. Rannacher. An optimal control approach to a posteriori error estimation in finite element methods. *Acta Numerica*, 10:1–102, 2001.

[5] H. Blum, D. Braess, and F. T. Suttmeier. A cascadic multigrid algorithm for variational inequalities. *Comput. Vis. Sci.*, 7(3-4):153–157, 2004.

[6] H. Blum, H. Ludwig, and A. Rademacher. Semi-smooth newton methods for mixed fem discretizations of higher-order for frictional, elasto-plastic two-body contact problems. *Ergebnisberichte Angewandte Mathematik, Fakultät für Mathematik, TU Dortmund*, 493, 2014.

[7] H. Blum, A. Schroeder, and F. Suttmeier. A posteriori estimates for FE-solutions of variational inequalities. In F. Brezzi and et al., editors, *Numerical mathematics and advanced applications. Proceedings of ENUMATH 2001, the 4th European conference, Ischia, July 2001*, pages 669–680, Berlin, 2003. Springer.

[8] H. Blum and F.-T. Suttmeier. An adaptive finite element discretisation for a simplified Signorini problem. *Calcolo*, 37(2):65–77, 2000.

[9] M. Braack and A. Ern. A posteriori control of modeling errors and discretization errors. *Multiscale Model. Simul.*, 1(2):221–238, 2003.

[10] D. Braess. A posteriori error estimators for obstacle problems – another look. *Numer. Math.*, 101(3):415–421, 2005.

[11] D. Braess, C. Carstensen, and R. Hoppe. Error reduction in adaptive finite element approximations of elliptic obstacle proplems. *J. Comput. Math.*, 27:148–169, 2009.

[12] D. Braess, C. Carstensen, and R. H. Hoppe. Convergence analysis of a conforming adaptive finite element method for an obstacle problem. *Numer. Math.*, 107(3):455–471, 2007.

[13] Z. Chen and R. H. Nochetto. Residual type a posteriori error estimates for elliptic obstacle problems. *Numer. Math.*, 84(4):527–548, 2000.

[14] P. Dörsek and J. Melenk. Adaptive hp-FEM for the contact problem with Tresca friction in linear elasticity: The primal-dual formulation and a posteriori error estimation. *Appl. Numer. Math.*, 60(7):689–704, 2010.

[15] G. Duvaut and J. L. Lions. *Inequalities in mechanics and physics*. Grundlehren der mathematischen Wissenschaften. Springer-Verlag, Berlin, 1976.

[16] I. Ekeland and R. Témam. *Convex analysis and variational problems*. Studies in Mathematics and its Applications. North-Holland Publishing Company, Amsterdam, 1976.

[17] J. Haslinger. Mixed formulation of elliptic variational inequalities and its approximation. *Apl. Math.*, 26:462–475, 1981.

[18] J. Haslinger and I. Hlávaček. Approximation of the Signorini problem with friction by a mixed finite element method. *J. Math. Anal. Appl.*, 86:99–122, 1982.

[19] P. Hild and S. Nicaise. A posteriori error estimations of residual type for Signorini's problem. *Numer. Math.*, 101(3):523–549, 2005.

[20] M. Hintermüller, K. Ito, and K. Kunisch. The primal-dual active set strategy as a semi-smooth newton method. *SIAM J. Optimization*, 13(3):865–888, 2003.

[21] R. Hoppe and R. Kornhuber. Adaptive multilevel methods for obstacle problems. *SIAM J. Numer. Anal.*, 31:301–323, 1994.

[22] S. Hüeber. *Discretization Techniques and Efficient Algorithms for Contact Problems.* PhD thesis, Universität Stuttgart, 2008.

[23] S. Hüeber, M. Mair, and B. Wohlmuth. A priori error estimates and an inexact primal-dual active set strategy for linear and quadratic finite elements applied to multibody contact problems. *Appl. Numer. Math.*, 54(3-4):555–576, 2005.

[24] C. Johnson. Adaptive finite element methods for the obstacle problem. *Math. Models Meth. Appl. Sci.*, 2:483–487, 1992.

[25] N. Kikuchi and J. Oden. *Contact problems in elasticity: A study of variational inequalities and finite element methods.* SIAM Studies in Applied Mathematics. SIAM, Society for Industrial and Applied Mathematics, Philadelphia, 1988.

[26] H. Kleemann. *Adaptive FEM für Mehrkörperkontaktprobleme.* PhD thesis, Technische Universität Dortmund, 2011.

[27] R. Kornhuber and R. Krause. Adaptive multigrid methods for Signorini's problem in linear elasticity. *Comput. Vis. Sci.*, 4(1):9–20, 2001.

[28] R. Krause, A. Veeser, and M. Walloth. An efficient and reliable residual-type a posteriori error estimator for the signorini problem. *Numer. Math.*, 2014. appeared online.

[29] R. Nochetto, K. Siebert, and A. Veeser. Pointwise a posteriori error control for elliptic obstacle problems. *Numer. Math.*, 95:163–195, 2003.

[30] M. Paraschivoiu, J. Peraire, and A. T. Patera. A posteriori finite element bounds for linear-functional outputs of elliptic partial differential equations. *Comput. Methods Appl. Mech. Engrg.*, 150(1-4):289–312, 1997.

[31] S. Prudhomme and J. Oden. On goal-oriented error estimation for elliptic problems: Application to the control of pointwise errors. *Comput. Methods Appl. Mech. Engrg.*, 176(1-4):313–331, 1999.

[32] A. Rademacher and A. Schröder. Dual weighted residual error control for frictional contact problems. Humboldt Universität zu Berlin, Institut für Mathematik, Preprint 12-07, 2012.

[33] T. Richter and T. Wick. Variational localizations of the dual-weighted residual estimator. *J. Comput. Appl. Math.*, 279:192–208, 2015.

[34] A. Schröder. Error control in h- and hp-adaptive FEM for Signorini's Problem. *J. Numer. Math.*, 17(4):299–318, 2009.

[35] A. Schröder, H. Blum, A. Rademacher, and H. Kleemann. Mixed FEM of higher order for contact Problems with friction. *Int. J. Numer. Anal. Model.*, 8(2):302–323, 2011.

[36] A. Schröder and A. Rademacher. Goal-oriented error control in adaptive mixed FEM for Signorini's Problem. *Comp. Meth. Appl. Mech. Engrg.*, 200(1-4):345–355, 2011.

[37] K. Siebert and A. Veeser. A unilaterally constrained quadratic minimization with adaptive finite elements. *SIAM J. Optim.*, 18:260–289, 2007.

[38] F. Suttmeier. *Numerical solution of variational inequalities by adaptive finite elements.* Advances in numerical mathematics. Vieweg-Teubner, Wiesbaden, 2008.

[39] A. Veeser. Efficient and reliable a posteriori error estimators for elliptic obstacle problems. *SIAM J. Numer. Anal.*, 39:146–167, 2001.

[40] A. Weiss and B. Wohlmuth. A posteriori error estimator and error control for contact problems. *Math. Comp.*, 78(267):1237–1267, 2009.

[41] B. I. Wohlmuth. An a posteriori error estimator for two-body contact problems on non-matching meshes. *J. Sci. Comput.*, 33(1):25–45, 2007.

[42] B. I. Wohlmuth and R. H. Krause. Monotone multigrid methods on nonmatching grids for nonlinear multibody contact problems. *SIAM J. Sci. Comput.*, 25(1):324–347, 2003.